

# LIGHT SCATTERING AT VARIOUS ANGLES

## THEORETICAL PREDICTIONS OF THE EFFECTS OF PARTICLE VOLUME CHANGES

PAUL LATIMER *and* B. E. PYLE

*From the Department of Physics, Auburn University, Auburn, Alabama 36830*

**ABSTRACT** The Mie theory of scattering is used to provide new information on how changes in particle volume, with no change in dry weight, should influence light scattering for various scattering angles and particle sizes. Many biological cells (e.g., algal cells, erythrocytes) and large subcellular structures (e.g., chloroplasts, mitochondria) in suspension undergo this type of reversible volume change, a change which is related to changes in the rates of cellular processes. A previous study examined the effects of such volume changes on total scattering. In this paper scattering at  $10^\circ$  is found to follow total scattering closely, but scattering at  $45^\circ$ ,  $90^\circ$ ,  $135^\circ$ , and  $170^\circ$  behaves differently. Small volume changes can cause very large observable changes in large angle scattering if the sample particles are uniform in size; however, the natural particle size heterogeneity of most samples would mask this effect. For heterogeneous samples of most particle size ranges, particle shrinkage is found to increase large angle scattering.

### INTRODUCTION

Many biological cells and large subcellular structures have been found to undergo large and reversible changes in their ability to scatter light (1-5). Most such optical changes are caused by particle swelling or shrinking. Particle volumes change by up to a factor of two. Water flows in or out of a particle while its dry weight remains constant. Active ion transport, which is coupled to processes such as photophosphorylation, takes place and water follows the ions. Similar volume changes also occur in response to changes in medium osmolarity. Optical techniques are very powerful tools for nondestructively following these changes in particle conformation. Such techniques are rapid, sensitive, and convenient; however, it is difficult to interpret reliably the observed changes in optical quantities without assistance from light-scattering theory.

We previously used the Mie theory to survey the influence on total scattering of changes in particle volume with no change in dry weight (4). Total scattering is *all* light, the direction of which has been changed by the sample. It might be reason-

able to expect total scattering and scattering at the various angles to change similarly. Exploratory theoretical calculations, however, revealed that volume changes influence scattering in the various directions differently. To provide a more comprehensive picture of how observable light fluxes should change when the sample particles swell or shrink with no change in dry weight, we provide new information on the effects of volume changes on scattering at 10° (forward scattering), 45°, 90°, 135°, and 170° (back scattering) from the incident beam.

### THEORETICAL APPROACH

The Mie equations, which are exact solutions of Maxwell's equations for isotropic homogeneous spheres, are used to calculate scattered light fluxes. Experimental tests of theoretical predictions of changes in total scattering, etc., revealed substantial theory-experiment agreement (5). These and related equations also have been shown to correctly predict absolute values of optical cross sections of erythrocytes, chloroplasts, yeast cells, *Escherichia coli* cells, and latex spheres (6-9). The angular dependences of scattering by yeast, *E. coli*, and cocci cells have also been shown to agree with theoretical predictions (10-14). Hence it is realistic to expect light-scattering equations, based on simple particle models, to correctly predict changes in observable scattered light fluxes by actual biological cells and subcellular structures.

The Mie equations (15, 16) give scattering in terms of the particle size parameter  $x$  and the relative complex index of refraction  $m$ , where  $x = 2\pi a/\lambda$ ,  $a$  is sphere radius,  $\lambda$  is the wavelength of the incident light in the medium,  $m = n - in'$  where  $n$  governs phase,  $n'$  is proportional to the absorption coefficient, and  $i = (-1)^{1/2}$ .

It is assumed that a biological cell or isolated subcellular structure behaves optically like a simple spherical sack of proteins and carbohydrates dissolved in water. Effects of the membrane and structural detail are neglected. Then if such particles take up or extrude medium (water), the expression for the refractive index of a solution gives

$$m = 1 + (m_o - 1)V_o/V, \quad (1)$$

where  $V$  is the particle volume, and the subscript  $o$  denotes initial or ordinary conditions. While equation 1 is an oversimplification, it is an adequate and convenient first approximation.

The relative roles of the particle size, scattering angle, and wavelength on observable light fluxes are suggested by the key parameter of the Rayleigh-Gans (Rayleigh-Debye) approximation:  $X = 2\sin(\theta/2)x \cong 2\pi a\theta/\lambda$ , where  $\theta$  is the scattering angle. Ideally the sample particles should be uniform in size, the photometer should be of high angular resolution, and the light beam should be spectrally pure. Monochromatic light is readily obtained; however, samples of cells or subcellular structures are usually heterogeneous in size. Furthermore the weakness of the scattered light usually requires the sacrifice of some angular resolution. Thus

meaningful calculations should account for effects of reasonable spreads in both  $a$  and  $\theta$ . In view of the complementary roles of  $a$  and  $\theta$  in  $X$ , however, an assumed spread in either quantity should give results equivalent to those for smaller spreads in both.

The incident light is assumed to be unpolarized. Then at each nominal scattering angle, e.g.  $\theta = 45^\circ$ , we assume a spread in  $\theta$  but not in  $a$ . The average intensity of the scattered light is assumed to be proportional to the weighted sum of the light scattered at three angles:

$$\text{Intensity} = c[I(\theta) \sin \theta + I(\theta + 5^\circ) \sin (\theta + 5^\circ) + I(\theta - 5^\circ) \sin (\theta - 5^\circ)], \quad (2)$$

where  $I(\theta)$  is the sum of the Mie intensities of the two polarization components of scattered light and  $c$  is a constant.

Observable scattered light intensities were calculated as functions of particle volume on the IBM 360-50 programmed in Fortran-IV. The Mie coefficients were calculated using Moore's scheme (17, 18). Nine representative particle sizes (0.002–4000  $\mu^3$ ) were used for illustrative calculations; the same sizes were previously used for Fig. 2 of reference 4. Assuming constant dry weight, scattering at the five different angles was calculated at volume intervals of 0.02  $V_o$  from 0.5  $V_o$  through 2.08  $V_o$ . For each particle size, scattering was calculated for a vacuum wavelength  $\lambda_o = 500 \text{ m}\mu^1$  (green light) assuming  $m_o = 1.05 - i 0.0$ . For most particles sizes, the calculations were repeated for  $\lambda_o = 1000 \text{ m}\mu$  (infrared light) and/or for  $m_o = 1.05 - i 0.015$  (absorbing particle) at 500  $\text{m}\mu$ . The vacuum refractive index of the medium, water, was assumed to be 1.336 so that if  $\lambda_o = 500 \text{ m}\mu$ ,  $x$  is evaluated using  $\lambda = 500/1.336 = 374 \text{ m}\mu$ .

## RESULTS OF CALCULATIONS

Figs. 1–5 show theoretical scattering intensities at five different scattering angles. The curves are for spheres of volumes which approximate those of the biological particles listed in Fig. 1. These curves illustrate how particle size, absorption coefficient, and wavelength influence scattering changes when particle volume increases or decreases. The curves of Fig. 1 for  $10^\circ$  scattering are seen to be relatively simple, while those for the larger angles are more complex.

The curves of Fig. 1 resemble those for total scattering by the same particles (4). Quantitatively, most of the light scattered by these particles appears at small angles. Then small angle scattering dominates total scattering. Increases in particle volume are seen to decrease  $10^\circ$  scattering for the smaller particles, and increase it for most of the larger ones. Wavelength and absorption coefficient have only minor effects on  $10^\circ$  scattering.

<sup>1</sup>  $\text{m}\mu$  is used here instead of the equivalent unit nm (nanometer) used in other papers in this issue.

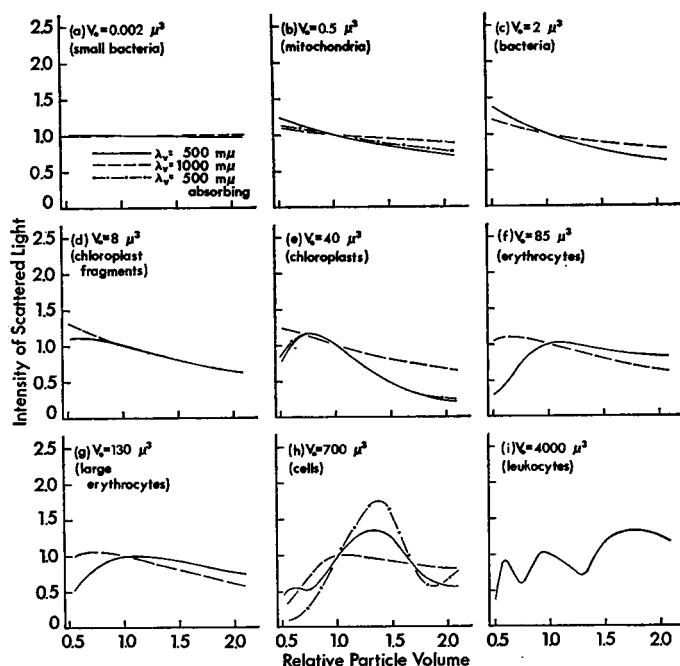


FIGURE 1 Scattering at  $10^\circ$  to the direction of the incident beam when particle volume  $V$  changes but dry weight remains constant (see equation 1). For all particles,  $n = 1.05$ . All curves are for spherical particles. Each plotted light intensity is effectively an average value over an assumed angular view of the photocell (see equation 2). Note that for  $V = 0.5 V_0$ ,  $a = 0.79 a_0$  and  $n = 1.10$ , while for  $V = 2.0 V_0$ ,  $a = 1.26 a_0$  and  $n = 1.025$ . (a) Small bacteria, (b) mitochondria, (c) bacteria, (d) chloroplast fragments, (e) chloroplasts, (f) erythrocytes, (g) large erythrocytes, (h) cells, (i) leukocytes.

Figs. 2–5 reveal that scattering at larger angles is more sensitive to changes in particle volumes. Here, especially, for the larger particle sizes and angles, the scattering curves have maxima and minima. While these illustrated curve structures are indeed dramatic, they represent only a fraction of the potential total structure because of the limited angular resolution of the photocell (see equation 2).

While the curve structure normally increases with both particle size and angle, the curve in Fig. 5 *i*, which is for the largest particle size and largest angle, has very little structure. In this case the inherent angular structure of the scattering pattern is finer than the assumed effective spread in the angular view of the photometer.

The figures reveal that doubling the wavelength frequently has a large effect. In terms of the size parameter  $x$ , the doubling of  $\lambda$  implies a reduction in effective particle radius to  $\frac{1}{2}$ , the effective volume to  $\frac{1}{8}$  of the original value. Absorption is seen to have only a small effect on scattering by small particles, and a larger effect on scattering by large particles.

All curves in these figures are normalized to an intensity of scattered light of 1.0

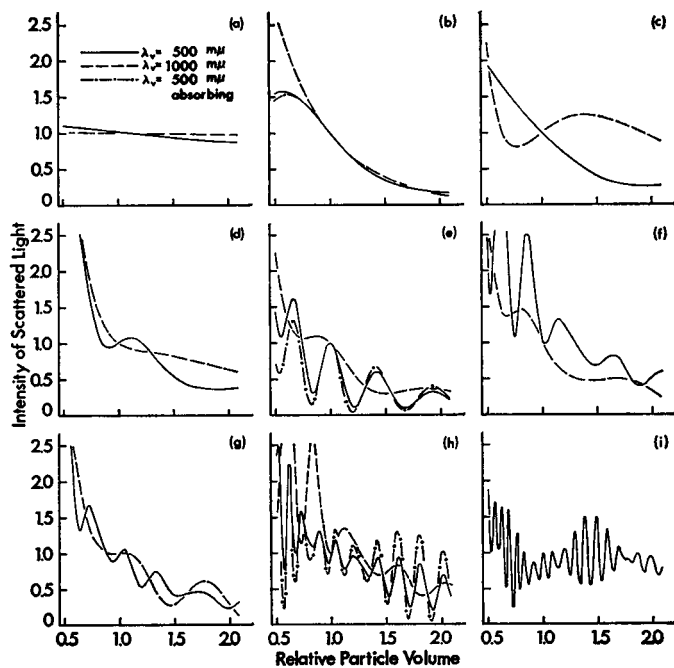


FIGURE 2 Scattering at  $45^\circ$  when particle volume changes but dry weight remains constant. The particle sizes of parts *a-i* are those of Fig. 1.

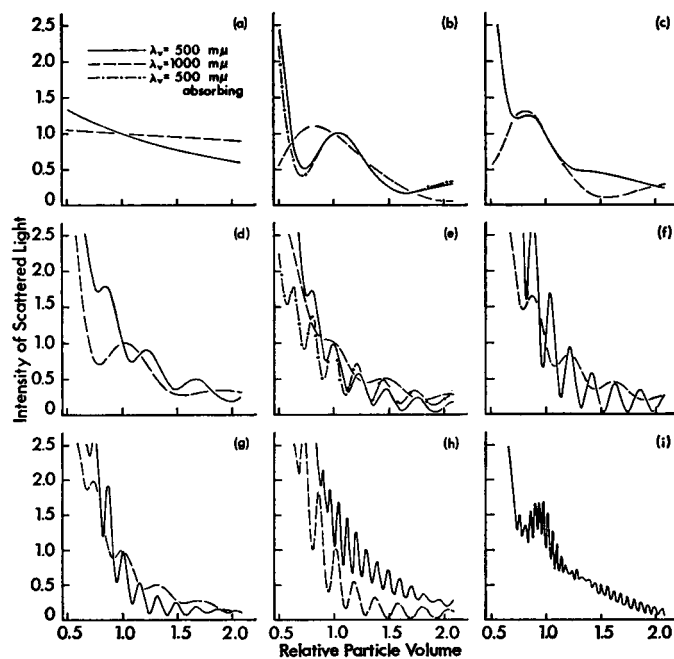


FIGURE 3 Scattering at  $90^\circ$  when particle volume changes but dry weight remains constant. The particle sizes for parts *a-i* are those of Fig. 1.

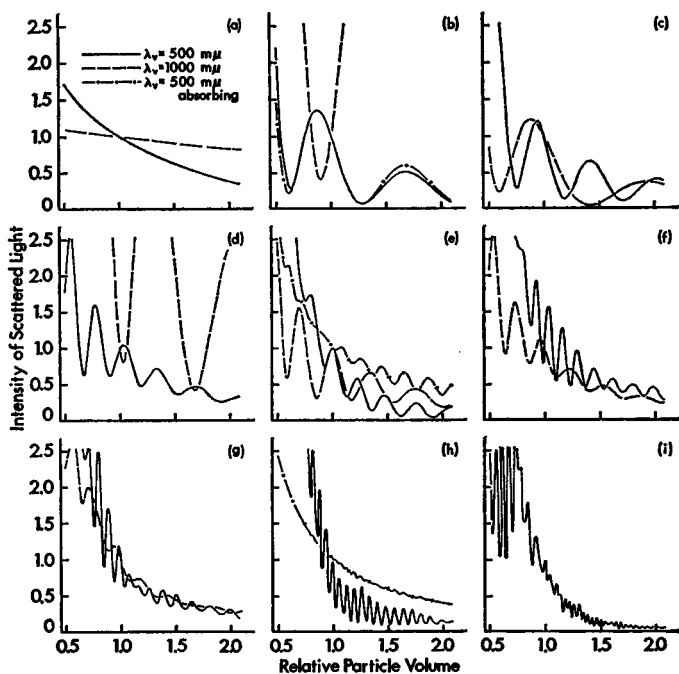


FIGURE 4 Scattering at  $135^\circ$  when particle volume changes but dry weight remains constant. The particle sizes for parts *a-i* are those of Fig. 1.

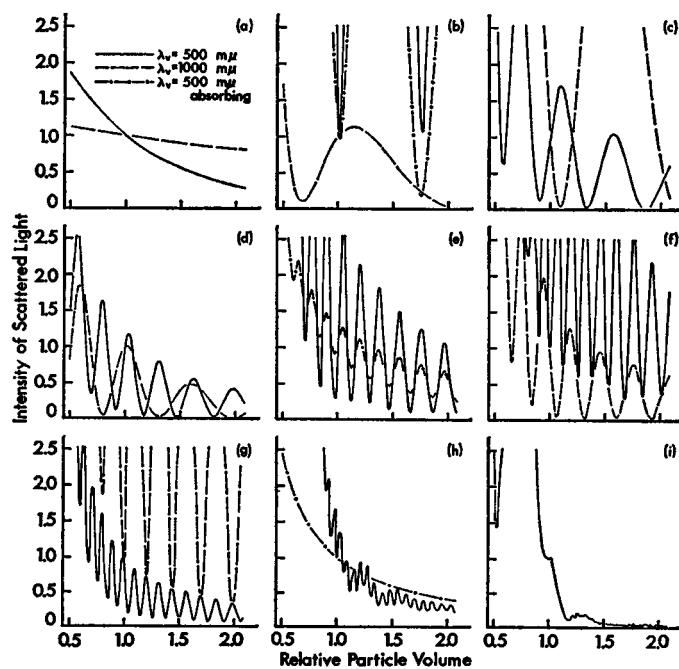


FIGURE 5 Scattering of  $170^\circ$  when particle volume changes but dry weight remains constant. The particle sizes for parts *a-i* are those of Fig. 1.

when  $V = V_0$ . This normalization causes most of the curves to lie near the center of the figure. For more structured curves, however, changes in volume induce large percentage changes in scattering levels (e.g., see Fig. 2 *f*). Then if a scattering minimum occurs at an angle close to the nominal angle, e.g.  $45^\circ$ , when  $V = V_0$ , the normalization at this point throws most of the scattering curve off scale (see Figs. 4 *b*, 4 *d*, 5 *b*, 5 *c*, and 5 *g*). These curves are basically no different from the others except that our normalization procedure raised them to very high levels.

## OPTICAL MECHANISMS

While the exact Mie equations are powerful tools for predicting light fluxes, optical approximations are the best source of physical pictures of the events. The well-known Rayleigh approximation describes scattering by particles of dimensions less than  $\lambda/10$ . Light senses such a particle essentially as a point. All elements of the particle scatter "in phase." Total scattering per particle is proportional to the square of the particle mass. The angular dependence of scattering is independent of particle size. Changes in the dimensions or shape of such a "point" particle leave it as a "point" of the same "magnitude" when dry weight is constant. Then conformational changes have essentially no influence on scattered light fluxes.

The Rayleigh-Gans (Rayleigh-Debye) approximation (15, 16) extends the domain of the Rayleigh theory to particles of dimensions of up to about  $\lambda$ . It corrects for destructive interference, in certain directions, of the light scattered from the different elements of a particle. If the particle is not too large, the primary effect of shrinkage is essentially to make it more pointlike. This reduces destructive interference at nonzero angles and thereby increases total scattering.

For particles larger than  $\lambda$ , diffraction theory can be used to describe small angle scattering. This scattering is closely related to single slit diffraction. Interference between light from the different parts of the slit is of prime importance in determining the angular scattering pattern (19). In diffraction theory, the scattered light is the sum, allowing for phase, of light which passes around the particle plus that which passes through it. The light which passes around the particle can be represented as that diffracted by an opaque circular obstacle. Light which passes through the particle can be represented as that diffracted by a circular opening in a baffle. According to Babinet's principle, the obstacle and opening produce complementary scattering patterns which completely cancel out, *except* insofar as the particle modifies the phase and amplitude of the light passing through it. For simplicity we presently use only one of these two wave fronts, not the sum, to represent scattering by diffraction. This neglects effects of phase shifts which should influence only the details of curve structure.

Both the Rayleigh-Gans and diffraction theories predict scattering maxima and minima at various angles. The  $x$  values of spheres for which the Rayleigh-Gans theory predicts scattering minima have been tabulated (15). From them we find

that, to a first approximation, scattering minima occur at angles

$$\theta \cong \frac{2k + 1}{2} \frac{\lambda}{d}, \quad (3)$$

where  $k$  is a positive integer and  $d$  is particle diameter. For larger particles diffraction theory (19) predicts scattering minima at angles which are approximated by a similar expression:

$$\theta \cong \frac{4k + 1}{4} \frac{\lambda}{d}. \quad (4)$$

These equations are similar to that for single slit diffraction:  $\theta = k\lambda/d$ . Note that, in these approximations, the locations of scattering minima depend on particle diameter and wavelength, not on refractive index.

A comparison of the scattering at specific angles in the present figures with total scattering by similar particles (see reference 4, Fig. 2) under the same conditions reveals that scattering at specific angles can undergo much larger changes. Actually as the particle swells, the scattering minima located by equations 3 and 4 move to smaller angles. A photometer observing light at a fixed angle reflects these changes in the angular scattering pattern as changes in the intensity of the scattered light. Observable light intensity at a given angle has a minimal value when a scattering minimum falls at the  $\theta$  of the photocell. Thus the large changes in scattering at certain angles seen in the figure are caused primarily by changes in the angular dependence of scattering, not by changes in total scattering.

### SCATTERING BY NONIDEAL SAMPLES

Typical samples of biological cells and subcellular structures are heterogeneous in particle size. Equations (3) and (4) reveal that such a heterogeneity should cause the intensity patterns for the various sizes to overlap. Then if all of the particles undergo similar volume changes, the scattered light received at a given angle from particles of some sizes would increase while that from particles of other sizes would decrease. The total observable scattered light would then change much more slowly than the component parts. If the size heterogeneity were sufficient to completely mask curve structure illustrated in the figures, the observable light fluxes would essentially follow the envelopes of the plotted curves. Interestingly, the envelopes of these curves display a systematic dependence on particle volume. With minor exceptions, particle shrinkage is seen to always increase the general level of scattering for  $\theta \geq 45^\circ$ .

In a recent study we examined the effects of varying the angular view of the photocell in transmission measurements. It was found (20) that total scattering at angles greater than  $30^\circ$  increases rapidly with particle refractive index, even when total



scattering at all angles remains relatively fixed. The envelopes of the curves in Figs. 2-5 indicate that the fluxes at these large angles behave in this way.

## DISCUSSION

Early studies (1, 2) of changes in scattering by biological cells and structures suggested that increases in large angle scattering or decreases in transmission imply particle shrinkage. Koch (21) offered theoretical support for this conclusion; however, in a more general treatment using the Mie theory (4), which yielded Koch's result as a special case, total scattering does, for some particle sizes, increase with particle shrinkage, but for most sizes, shrinkage decreases total scattering. Since shrinkage is presently found to increase large angle scattering if the sample is heterogeneous, large angle scattering and total scattering must frequently change in opposite directions.

In our previous study (4) it was shown that certain effects of internal particle structure could cause total scattering and large angle scattering to change in opposition. Note that all of the present findings are for homogeneous spheres with no internal structure. The present opposite changes in scattered light fluxes are not related to the previous ones.

The Mie equations predict scattering by a homogeneous sphere from two parameters,  $x$  and  $m$ . While they are independent variables in these equations, this study considers only the special case where both are functions of particle volume. It was previously shown that these two parameters control total scattering almost exclusively through the variable  $\rho^* = 2x(m - 1)$ . Scattering at  $10^\circ$  is now found to be controlled by the same quantity; however, the manner in which  $x$  and  $m$  separately influence large angle scattering is different. The size parameter  $x$  controls details of the angular scattering pattern. It is responsible for the structure of the curves in our figures. On the other hand,  $m$  influences the general level of large angle scattering.

In conclusion, illustrative calculations have revealed the basic functional dependence of changes in particle volume, with no change in dry weight, on light scattered at various angles. The results indicate that the light scattered at different angles contains distinctive information about the sample particle. Empirical evidence has previously given some basis for interpreting scattering changes in terms of changes in particle volume. Theoretical studies such as this one improve our understanding of the optical changes. Hopefully, this will enhance the capability, reliability, and usefulness of the optical techniques.

We thank Dr. Paul Budenstein, Mr. Pat Graham, and Mrs. Rose Porter for assistance with the manuscript and the Auburn University Computer Center for computer time. Finally, we cordially acknowledge earlier helpful advice, encouragement, and penetrating questions from Dr. Eugene I. Rabinowitch.

*Received for publication 19 April 1971.*

## REFERENCES

1. CLELAND, K. W. 1952. *Nature (Lond.)* **170**:497.
2. PACKER, L. 1963. *Biochim. Biophys. Acta.* **75**:12.
3. BORN, G. V. R., and M. HUME. 1967. *Nature (Lond.)* **215**:1027.
4. LATIMER, P., D. M. MOORE, and F. D. BRYANT. 1968. *J. Theor. Biol.* **21**:348.
5. BRYANT, F. D., P. LATIMER, and B. A. SEIBER. 1969. *Arch. Biochem. Biophys.* **135**:109.
6. MACRAE, R. A., J. A. MCCLURE, and P. LATIMER. 1961. *J. Opt. Soc. Am.* **51**:1366.
7. LATIMER, P., and C. A. H. EUBANKS. 1962. *Arch. Biochem. Biophys.* **98**:274.
8. BRYANT, F. D., B. A. SEIBER, and P. LATIMER. 1969. *Arch. Biochem. Biophys.* **135**:97.
9. SEIBER, B. A., and P. LATIMER. 1967. *J. Colloid Interface Sci.* **23**:509.
10. LATIMER, P., and B. TULLY. 1968. *J. Colloid Interface Sci.* **27**:475.
11. KOCH, A. L., and E. EHRENFELD. 1968. *Biochim. Biophys. Acta.* **165**:262.
12. WYATT, P. 1970. *Nature (Lond.)*. **226**:277.
13. TULLY, D. B. 1970. Multiple scattering effects on small angle light scattering. M.S. Thesis. Auburn University, Auburn, Ala.
14. CROSS, D. A., and P. LATIMER. 1972. *Appl. Opt.* **11**:1225.
15. VAN DE HULST, H. C. 1957. *Light Scattering by Small Particles*. John Wiley & Sons, Inc., New York.
16. KERKER, M. 1969. *The Scattering of Light*. Academic Press, Inc., New York.
17. MOORE, D. M., F. D. BRYANT, and P. LATIMER. 1968. *J. Opt. Soc. Am.* **58**:281.
18. MOORE, J. D. 1968. M.S. Thesis. Auburn University, Auburn, Ala.
19. JENKINS, F. A., and H. E. WHITE. 1957. *Fundamentals of Optics*. McGraw-Hill Book Company, New York. 3rd edition. 294-304.
20. LATIMER, P. 1972. *J. Opt. Soc. Am.* **62**:208.
21. KOCH, A. L. 1961. *Biochim. Biophys. Acta.* **51**:429.